ORIGINAL ARTICLE

lajss.org Latin American Journal of Solids and Structures

www.lajss.org

# Mechanical Mechanism Analysis and Influencing Factors of Subway Cross Passage Construction

**Wu Ke**[a]

**Cui Shuaishuai**[a]*

**Zhang Qianjin**[a]

**Zhang Zheng**[a]

**Zhao Jiahui**[a]

**Yu Yalin**[a]

[a] School of Civil Engineering, Shandong University, Jinan, China. E-mail: wuke@sdu.edu.cn, 2018567179@qq.com, 861612589@qq.com, 1281820587@qq.com, 978715768@qq.com, 825516736@qq.com

* Corresponding author

http://dx.doi.org/10.1590/1679-78255512

**Abstract**

The construction of the cross passage changes the main tunnels segment from a complete cylindrical structure to a notched unstable stressed structure. Thus, the overall force (bending and shearing) performance of the main tunnels is considerably decreased. The excavation of the cross passage also destroys the stability of the original soil layer and main tunnels and causes difficulty in avoiding the settlement of the surface and main tunnels. Numerical simulation analysis of the mechanical characteristics and influencing factors analysis were carried out using FLAC3D. Results show that (1) the construction of the cross passage largely disturbs the main tunnels. The settlement of the intersection part of the main tunnels and cross passage is mainly concentrated from −7 m to 7 m. (2) During the construction of the cross passage, the original main tunnels are subjected to stress redistribution, which causes stress concentration in the intersecting segments, especially in the opening side segment has an unfavorable force form in which the upper and lower sections are integrally pulled. (3) The construction of the cross passage causes a large tensile stress area in the structure as well. As a result, the overall tension of the upper and lower sections of the structure and the compression of the hance are unfavorable. (4) The influence of the excavation of the cross passage on the surface and main tunnels is related to the buried depth, intersection angle, excavation method, and grouting range. Therefore, the influence of different parameters can be analyzed by changing the model parameters.

**Keywords**

subway; cross passage; main tunnels; numerical simulation; construction mechanism; influencing factors

## 1 INTRODUCTION

The cross passage in the middle of the main tunnels plays the roles of connecting two tunnels, collecting, draining, fire preventing, and evacuating [1-4]. The cross-section span of the cross passage is generally 2.0–3.0 m, the height of the wall is 2.5–4.0 m, and the section is rectangular, circular, or straight wall arched [5-7]. The construction of the cross passage changes the main tunnels segment from a complete cylindrical structure to an unstable force structure with notches; thus, the overall force (bending and shearing) performance of the tunnel is considerably decreased [8-11]. After the support construction of the cross passage, the tunnel and cross passage form a 3D complex intersection structure[12-14]. The excavation of the cross

Received: February 19, 2019. In Revised Form: May 14, 2019. Accepted: May 19, 2019. Available online: May 20, 2019.
http://dx.doi.org/10.1590/1679-78255512

passage also destroys the stability of the original soil layer and the main tunnels and causes difficulty in avoiding the settlement of the surface and the displacement of the main tunnels[15]. The influence of the excavation of the cross passage on the surface and main tunnels is related to the overlying soil thickness, intersection angle, excavation method, and grouting range. Therefore, the influence of different parameters can be analyzed by changing the physical parameters of the model.

Accurate analysis of the mechanical behavior of the surrounding rock and the change of the main tunnels during the construction of the cross passage is the primary prerequisite and necessary condition to ensure the safe, rapid, and economical construction of the cross passage[16]. Domestic and foreign scholars have conducted considerable research on the cross passage. Yang Wu [17] introduced the risk control measures of the cross passage in the construction of Shanghai Metro Line 8 in 2011. Wang Shimin et al. [18] studied the cross passage and water-collecting well of Wuhan Metro Cross of Yangtze River Tunnel in the middle section of the Yangtze River in 2012. A numerical simulation method for the mechanical behavior of underground structure under the condition of high water pressure in sandy stratum was proposed, and the deformation and stress of the lining of the steel tube sheet, connection passage, and water-collecting well were obtained. Key factors of distribution were also determined. Liu Jun et al. [19] applied numerical simulation method to study the mechanical behavior of the segment during the construction of a shield tunnel cross passage in Beijing Metro. Through on-site monitoring analysis and 3D finite element numerical analysis of the mechanical behavior of the segment during the construction of the cross passage, the construction process and segment opening were obtained. The stress and displacement characteristics of the segment were also determined.

At present, most studies on subway cross passage concentrate on the stress characteristics of the segments during the construction of the cross passage and do not perform influencing factors analysis. In this study, the mechanical characteristics of the construction of the subway cross passage are analyzed using Fast Lagrangian Analysis of Continua in 3 Dimensions (FLAC3D) numerical simulation software. Then, the influencing factors such as buried depth, intersection angle, excavation method, and grouting range are analyzed.

## 2 Numerical calculation models and methods

### 2.1 Project overview

The earth pressure balance shield is used to construct the left and right lines of the main tunnels in subway. The outer diameter of the shield tunnel is 6.0 m, and the inner diameter is 5.4 m. The buried depth of the main tunnels is 9 m. The cross passage is constructed by the full-face excavation with a length of 10 m, a width of 3 m, a height of 4.3 m, and the thickness of lining is 0.2 m. The cross passage is excavated from both sides to the middle simultaneously to accelerate the construction speed.

### 2.2 Numerical calculation model

In accordance with the geological report and the actual engineering situation, FLAC3D is used to establish the 3D model and calculation. In the model, the cross passage excavation section width B=3 m and the angle of the main tunnels and cross passage is 90°. To consider the related size effect, the distance from the model edge to the main tunnels edge is five times larger than the tunnel diameter and the distance from the bottom boundary to the tunnel bottom is greater than 4 times the tunnel height. The model is 60 m in length, 70 m in width, and 47 m in height. The final numerical model is shown in Figure 1. The model is divided into 82315 elements and 77546 nodes.

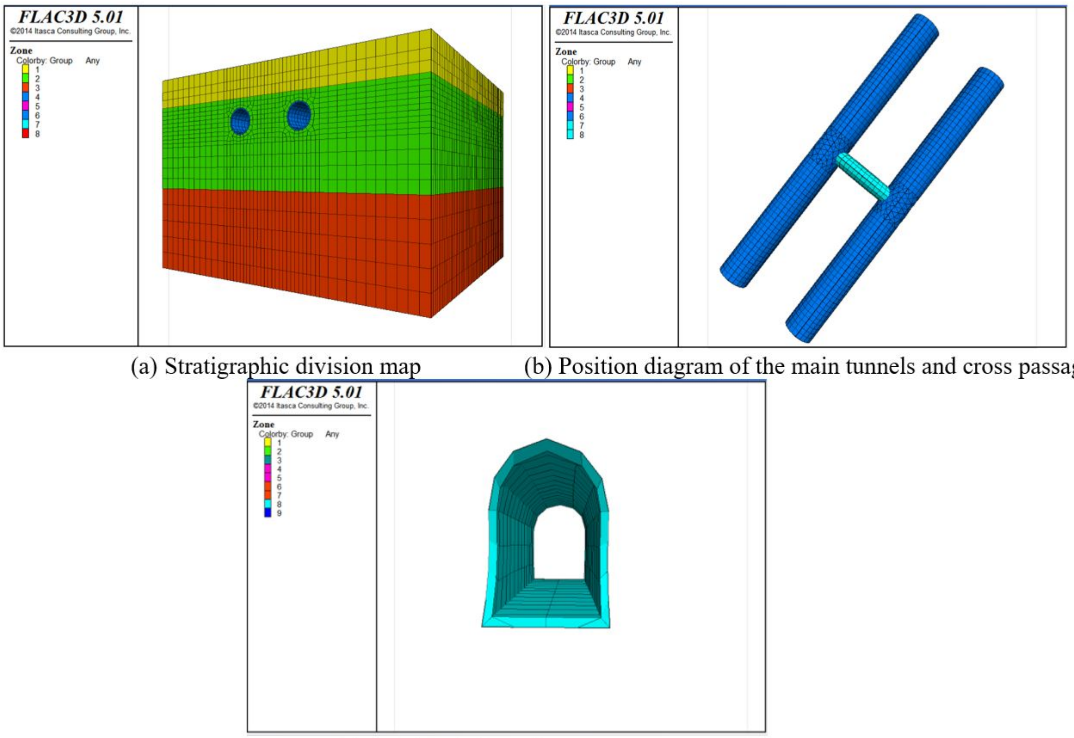


(a) Stratigraphic division map (b) Position diagram of the main tunnels and cross passage

(c) Sectional view of cross passage

**Figure 1.** Model diagram

## 2.3 Numerical analysis method

The specific numerical analysis methods are listed as follows:

1)Boundary conditions: set normal direction displacement constraints on the left, right, front and rear boundary of the model, the top of the surrounding rock mass is the free surface, set vertical displacement constraint at the bottom boundary of the model.

2)Loads are applied by gravity, and grouting layer is simulated by improving the formation parameters. The shell element is used to simulate the support structure, and the solid element is used to simulate the surrounding rock.

3)Excavation method: Full-face excavation is adopted, and excavation is carried out from both sides. The excavation footage is 2 m, that is, 2 m are excavated in one cycle.

4)Calculation steps:

① Stress is balanced.

② The left and right segments are removed as excavation step 1.

③ The soil on both sides is excavated and the initial supports are applied, which are divided into excavation steps 2-4.

## 2.4 Material parameters

The material properties used in the numerical calculation are shown in Table 1.

**Table 1** Mechanical properties of geotechnical material

| Material | Density /(Kg· m$^{-3}$) | Bulk Modulus / MPa | Shear Modulus / MPa | Cohesion /KPa | Friction angle /(°) |
|---|---|---|---|---|---|
| **Plain fill** | 1,600 | 5 | 6 | 10 | 12 |
| **Gravel clay** | 1,860 | 18 | 9 | 26 | 20 |
| **Grouting zone** | 2,100 | 32 | 15 | 32 | 25 |
| **Strongly weathered granite** | 2,040 | 47 | 29 | 45 | 25 |
| **Support** | 2,500 | 14,800 | 12,000 | - | - |

### 2.5 Reliability verification of numerical analysis

Figure 2 shows the layout of monitoring points for ground settlement, and Figure 3 is the surface settlement curve. The numerical simulation results shows that the maximum settlement value of the cross passage monitoring section is 5.09 mm, and the maximum value occurs above the cross passage axis. The data obtained from field monitoring show that the maximum value of ground settlement is 5.92 mm. The comparison of numerical simulation results and field monitoring data shows the position of the maximum point of ground settlement is the same. The calculation result of the maximum value of ground settlement is close to the field monitoring result. The maximum error between the simulated and measured values is 14%. From the scope of influence, the two have good similarity, which shows that the numerical calculation method used in this study is close to the actual project. The calculation results also have a certain degree of reliability.

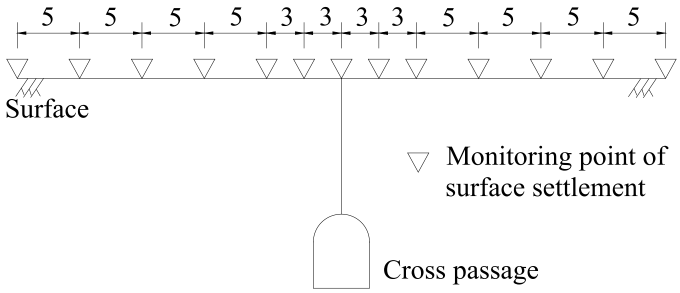


**Figure 2.** Monitoring point layout of the surface settlement

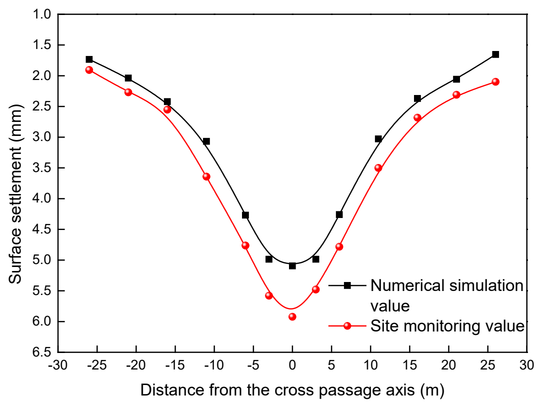


**Figure 3.** Surface settlement curve along the centerline of the two main tunnelss

## 3 Mechanical Mechanism Analysis

### 3.1 Settlement analysis

(1) Surface settlement

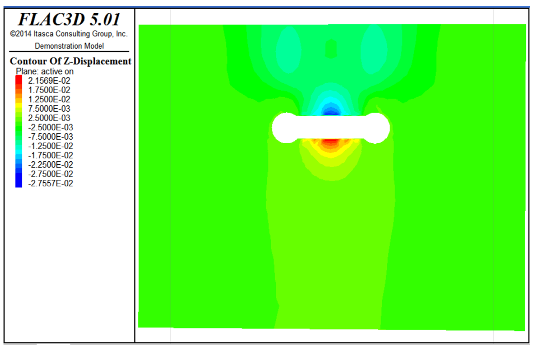


**Figure 4** Stratum settlement cloud picture

The cloud picture of stratum settlement after the construction of cross passage is shown in Figure 4. The curves of surface horizontal settlement along the axis of the main tunnels and the centerline of the two main tunnels are shown in Figures 5(a) and 5(b), respectively. It can be seen from the figures that when the construction of the cross passage is completed, the cumulative settlement of the surface at the midline position between the two tunnels and above main tunnel axis have become the largest. The horizontal settlement curve of the surface caused by the excavation of the cross passage is U-shaped. As the excavation proceeds, the surface settlement increases gradually. For the surface settlement along the axis of the main tunnels, the difference of surface settlement is the largest under excavation step 4. For the surface settlement along the centerline between the two main tunnels, large differences are observed in surface settlement under excavation steps 3 and 4. With the excavation of the cross passage, the ground surface will have a continuous settlement process. When the construction of the cross passage is completed, the cumulative surface settlement at the centerline between the two tunnels becomes the largest, and the maximum ground settlement is 5.09 mm.

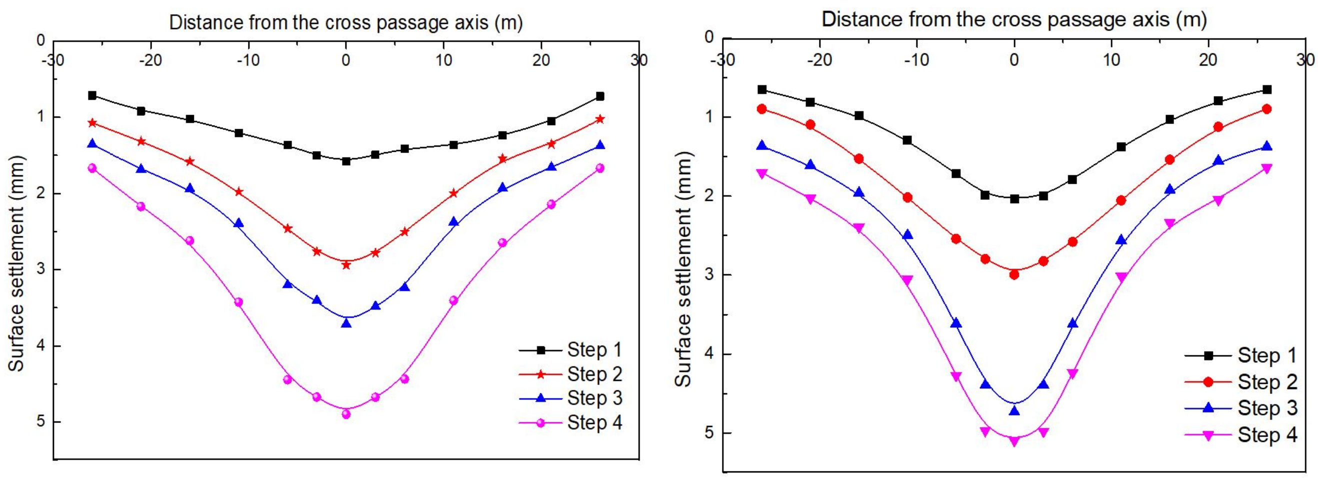


(a) Along the main tunnel axis (b) Along the centerline of the two main tunnels

**Figure 5** Surface settlement curve

(2) Settlement of main tunnels

The excavation steps are analyzed separately to understand the influence of the cross passage construction on the settlement of the main tunnels. As shown in Figure 6, the settlement curves of the tunnel lining at different excavation steps are U-shaped, and the main tunnels will have a continuing process of settlement when the cross passage is excavated. When excavation step 1 is completed (removing the left and right segments of the main tunnels), the segment near the intersection of the main tunnels and cross passage will generate settlement, and the maximum settlement value is 1.12 mm. When excavation step 4 is finished, the construction of the cross passage is completed, and the maximum vault settlement of the main tunnels is 3.93 mm. As can be seen from the figure, the maximum settlement of the main tunnel is increased by 2.5 times from the start of cross passage construction to the completion of cross passage construction. At the same time, it can be seen that the uneven settlement of the main tunnel has changed from 0.85mm to 1.42mm. Thus, the corresponding reinforcement measures should be taken to ensure the stability of the main tunnels, such as grouting reinforcement and freezing construction. The settlement under each excavation step is mainly concentrated from −7 m to 7 m of the intersection of the main tunnels and cross passage. Therefore, attention should be paid to these parts during reinforcement.

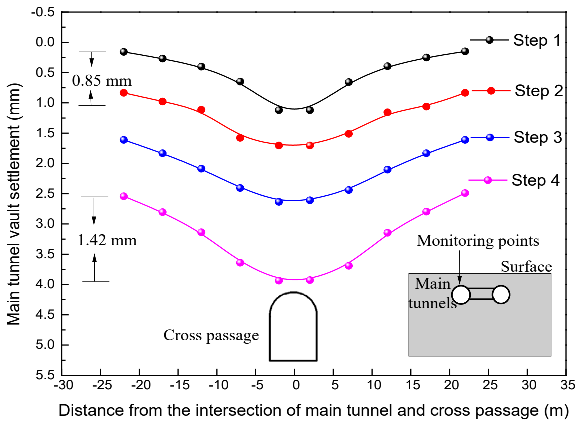


**Figure 6** Vault settlement curve of the left main tunnels

(3) Horizontal convergence of main tunnels

The horizontal convergence curve of the main tunnels during the construction of the cross passage is shown in Figure 7. The figure shows that the convergence curve of the tunnel segment at different excavation steps is "U" type, and the convergence mainly concentrates from −7 m to 7 m of the intersection of the main tunnels and cross passage. The excavation of the cross passage will cause the horizontal displacement of the main tunnels segment outside of the main tunnels, and the position of the maximum displacement is located at the intersection of the cross passage. With the excavation of the cross passage, the horizontal convergence value of the main tunnels increases continuously. When excavation step 1 is completed, the maximum convergence value of the main tunnels is 1.84 mm. When excavation step 4 is finished, the construction of the cross passage is completed, and the maximum convergence value of the main tunnels is 2.74 mm.

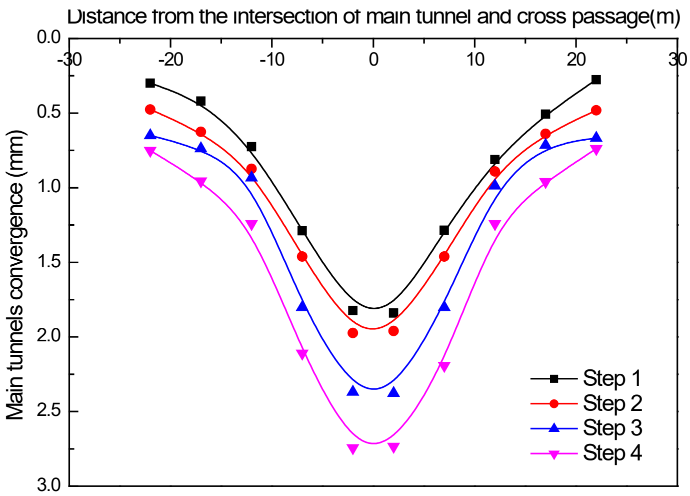


**Figure 7.** Horizontal convergence curve of the left main tunnel

### 3.2 Stress analysis

The maximum and minimum principal stress cloud pictures of the main tunnels and cross passage are shown in Figures 8 and 9, respectively.

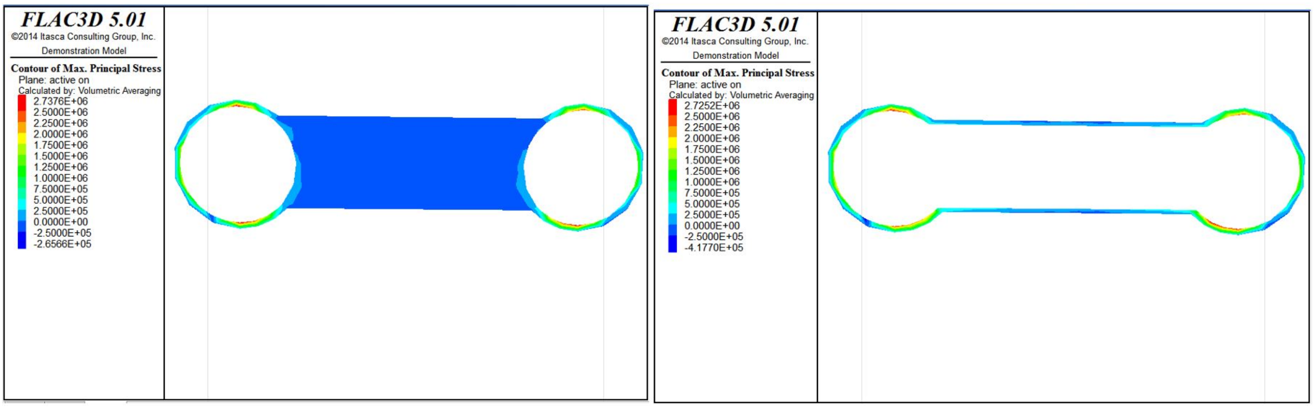


**Figure 8** Horizontal convergence curve of the left main tunnel

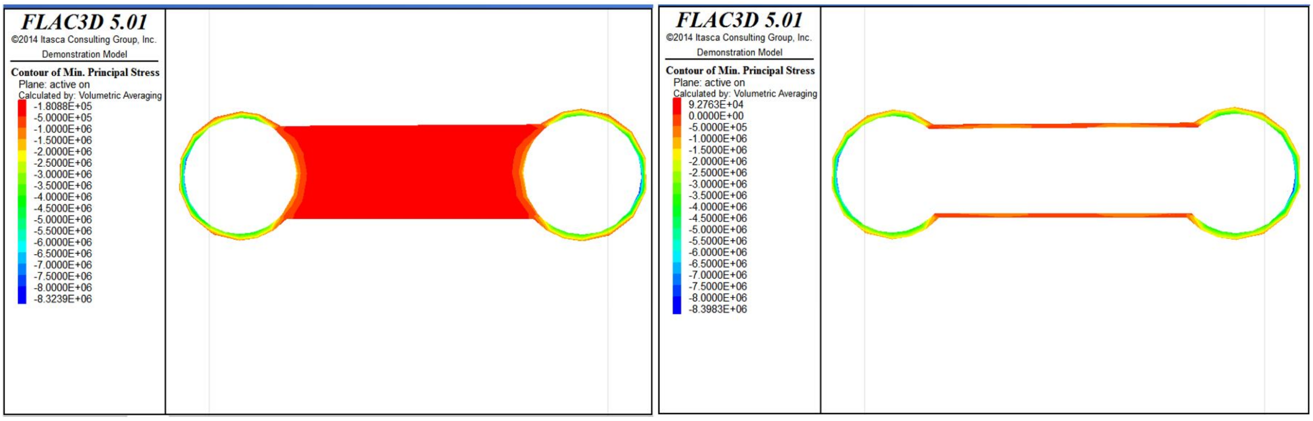


**Figure 9** Minimum principal stress cloud picture (Pa)

(1) Stress of main tunnels

The maximum and minimum principal stress distributions of the main tunnels are shown in Tables 2 and 3, respectively. Combined with the principal stress cloud picture, the results show that large tensile stresses appear in the vault and bottom of the main tunnels, the maximum tensile stress of the vault is 2.73 MPa, and the maximum compressive stress of the tunnel appears at the hance on the opposite side of the opening segment before the construction of the cross passage. The maximum compressive stress is 8.40 MPa. The construction of the cross passage increases the tensile stress of the segment at the intersection of the opening side in varying degrees. However, the compressive stress of the segment at the intersection of the opening side decreases with the construction progresses, and the compressive stress on the opposite hance of the opening segment increases gradually. As the cross passage is constructed, the stress redistribution occurs in the intersection segment, especially in the opening side segment. Ultimately, an unfavorable form of force that is pulled up by the upper and lower sections is produced. Therefore, the intersection part should be reinforced effectively and sufficient support should be implemented during construction.

**Table 2** Maximum principal stress of the main tunnels segment (Mpa)

| Construction step | Tensile stress | | Compressive stress | |
|---|---|---|---|---|
| | Maximum | Location | Maximum | Location |
| **Initial stress** | 2.23 | Vault | 0.27 | Hance on the opposite side of the opening segment |
| **Step 1** | 2.46 | Top of opening side | 0.32 | Hance on the opposite side of the opening segment |
| **Step 2** | 2.57 | Top of opening side | 0.36 | Hance on the opposite side of the opening segment |
| **Step 3** | 2.63 | Top of opening side | 0.40 | Hance on the opposite side of the opening segment |
| **Step 4** | 2.73 | Top of opening side | 0.42 | Hance on the opposite side of the opening segment |

**Table 3** Minimum principal stress of the main tunnels segment (Mpa)

| Construction step | Compressive stress | |
|---|---|---|
| | Maximum | Location |
| Initial stress | 8.21 | Hance on the opposite side of the opening segment |
| Step 1 | 8.22 | Hance on the opposite side of the opening segment |
| Step 2 | 8.27 | Hance on the opposite side of the opening segment |
| Step 3 | 8.37 | Hance on the opposite side of the opening segment |
| Step 4 | 8.40 | Hance on the opposite side of the opening segment |

The maximum and minimum principal stress distributions of the cross passage are shown in Tables 4 and 5, respectively. The earth pressure balance shield is used to construct the left and right lines of the main tunnels in subway. The outer diameter of the shield tunnel is 6.0 m, and the inner diameter is 5.4 m. The buried depth of the main tunnels is 9 m. The cross passage is constructed by the full-face excavation with a length of 10 m, a width of 3 m, a height of 4.3 m, and the thickness of lining is 0.2 m. The cross passage is excavated from both sides to the middle simultaneously to accelerate the construction speed.

**Table 4** Maximum principal stress of cross passage segments (Mpa)

| Construction step | Tensile stress | | Compressive stress | |
|---|---|---|---|---|
| | Maximum | Location | Maximum | Location |
| Initial stress | 0.65 | Hance | 0.25 | Bottom |
| Step 1 | 1.13 | Bottom | 0.17 | Hance |
| Step 2 | 1.28 | Bottom | 0.14 | Hance |
| Step 3 | 1.41 | Bottom | 0.11 | Hance |
| Step 4 | 1.47 | Bottom | 0.08 | Hance |

**Table 5** Minimum principal stress of cross passage segments (Mpa)

| Construction step | Compressive stress | |
|---|---|---|
| | Maximum | Location |
| Initial stress | 5.01 | Hance |
| Step 1 | 6.01 | Hance |
| Step 2 | 6.09 | Hance |
| Step 3 | 6.16 | Hance |
| Step 4 | 6.22 | Hance |

## 4 Influencing factors

In the cross passage construction project, many factors affect the deformation of the main tunnels, and the influence law of each factor is complicated. Therefore, this section uses the numerical simulation method based on a cross passage construction project and analyzes the influence law of the buried depth, intersection angle, construction method, and grouting range on the surface and main tunnels.

### 4.1 Buried depth

The modeling conditions of four different buried depth (distance from the main tunnels vault to the surface) are selected for modeling to consider the influence of cross passage construction on existing main tunnels. The specific operating condition parameters are shown in Table 6, and models are shown in Table 7.

**Table 6** Different buried depths

| Working condition | Buried depth (m) | Intersection angle | Main tunnels type | Construction method of cross passage |
|---|---|---|---|---|
| 1 | 6 | 90° | Shield tunnel | Full-face excavation |
| 2 | 9 | 90° | Shield tunnel | Full-face excavation |
| 3 | 12 | 90° | Shield tunnel | Full-face excavation |
| 4 | 15 | 90° | Shield tunnel | Full-face excavation |

**Table 7** Grouting range diagram

| Working condition | Working condition 1 | Working condition 2 | Working condition 3 | Working condition 4 |
|---|---|---|---|---|
| Model | 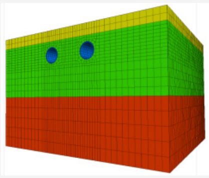 | 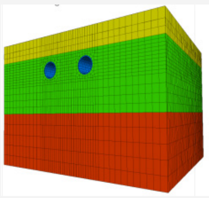 | 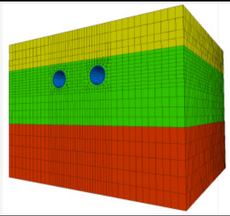 | 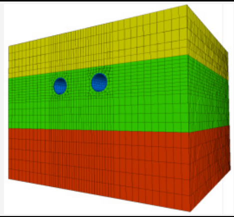 |

The settlement cloud picture under different buried depth conditions is shown in Figure 10. The figure shows that the maximum surface settlements under the four conditions are 2.61, 5.09, 7.38, and 10.13 mm and occur directly above the main tunnels. The maximum settlements of the main tunnels vault are 2.87, 3.93, 4.78, and 5.66 mm. The maximum horizontal convergence values of the main tunnels are 2.21, 2.74, 3.25, and 3.89 m. The maximum settlements of the cross passage are 5.29, 10.15, 15.01, and 21.95 mm and occur near the vault of the cross passage. The deformation values under different buried depth are merged into a curve, as shown in Figure 11(a). The figure indicates that the horizontal convergence of the main tunnels and the settlements of the main tunnels, ground surface, and vault of the cross passage increase with the increase in the thickness of the overlying soil. Moreover, the linear correlation is significant.

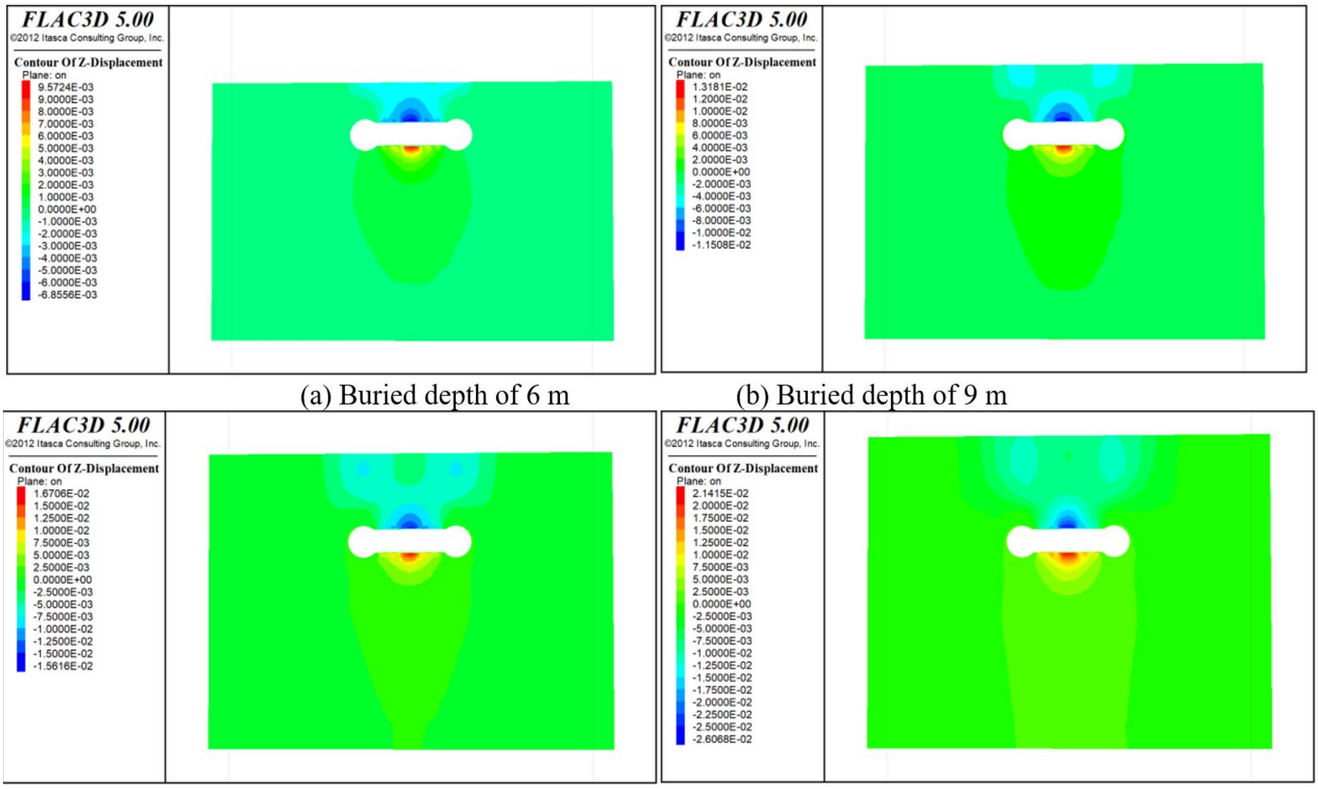


(a) Buried depth of 6 m (b) Buried depth of 9 m

(c) Buried depth of 12 m (d) Buried depth of 15 m

**Figure 10** Surface settlement under different buried depths

The maximum tensile stresses of the main tunnels are 1.15, 1.66, 2.16, and 2.59 Mpa and occur in the main tunnels vault. The minimum principal compressive stresses of the main tunnels are 4.19, 5.64, 7.11, and 8.44 Mpa and occur near the hance on the opposite side of the opening segment. Figure 11(b) shows the variation in the stress value of the main tunnels under different buried depths. As shown in the figure, the maximum and minimum principal stresses of the main tunnels increase with the increase in the buried depth. The linear correlation is significant.

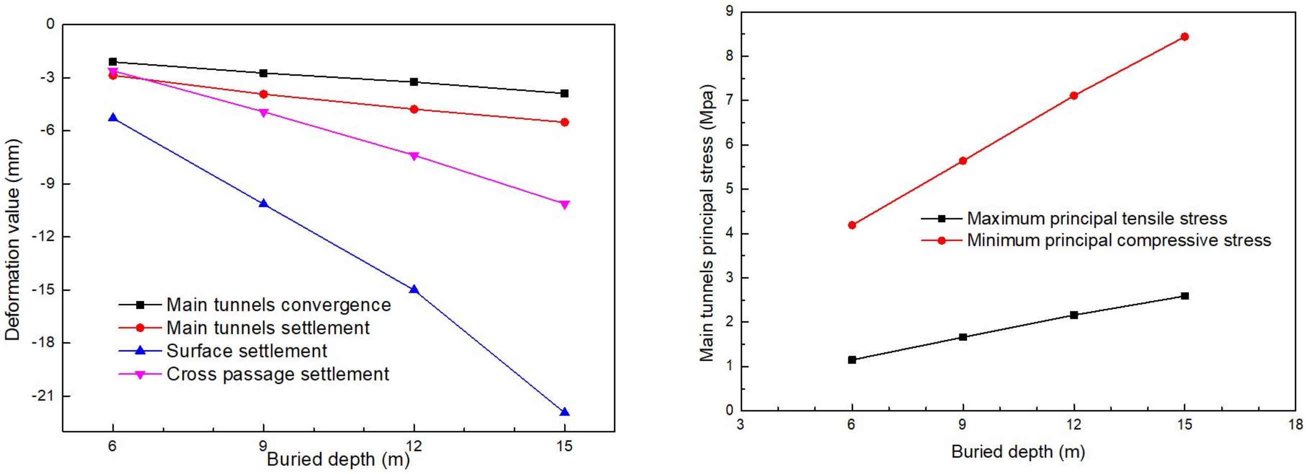


(a) Deformation (b) Stress

**Figure 11** Variations under different buried depths

### 4.2 Intersection angle

The working conditions under four different intersection angles are selected for modeling and analysis to consider the influence of the construction of the cross passage on the existing main tunnels. The specific working conditions are shown in Table 8, and the model diagram is shown in Table 9.

**Table 8** Different intersection angles

| Working condition | Buried depth (m) | Intersection angle | Main tunnels type | Construction method of cross passage |
|---|---|---|---|---|
| 1 | 9 | 45° | shield tunnel | full-face excavation |
| 2 | 9 | 60° | shield tunnel | full-face excavation |
| 3 | 9 | 75° | shield tunnel | full-face excavation |
| 4 | 9 | 90° | shield tunnel | full-face excavation |

**Table 9** Models with different intersection angles

| Working condition | Working condition 1 | Working condition 2 | Working condition 3 | Working condition 4 |
|---|---|---|---|---|
| Model | 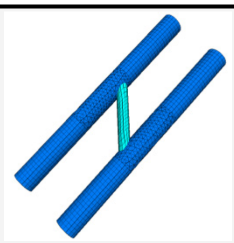 | 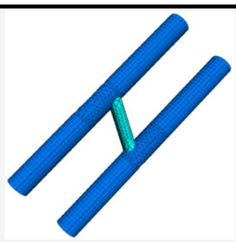 | 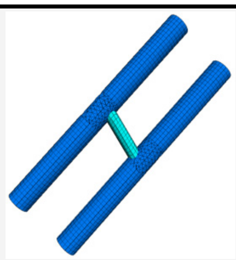 | 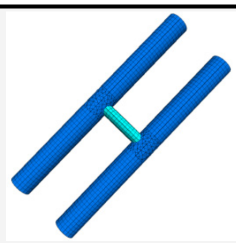 |

The surface settlement under different intersecting angle conditions is shown in Figure 12. The figure shows that the surface settlement values are roughly distributed near the surface above the main tunnels and cross passage under different intersecting angles. A small intersection angle indicates large distribution of the blue region. That is, the small uneven settlement of the surface is mainly due to the smaller the angle, the larger area of the intersection zone. Figure 12 also shows that the maximum settlement value of the ground surface is the smallest with 4.64 mm when the intersection angle is 45°. When the intersection angle is larger than 45°, the area affected by the intersection of the cross passage and main tunnels stabilizes. The intersection area is also rapidly decreased compared with the case in which the intersection angle is 45°. Therefore, the maximum settlement value of the surface at this time is larger than the intersection angle of 45°, and the variation range of the maximum settlement value considerably decreases, stabilizes, and is scattered at approximately 5.10 mm.

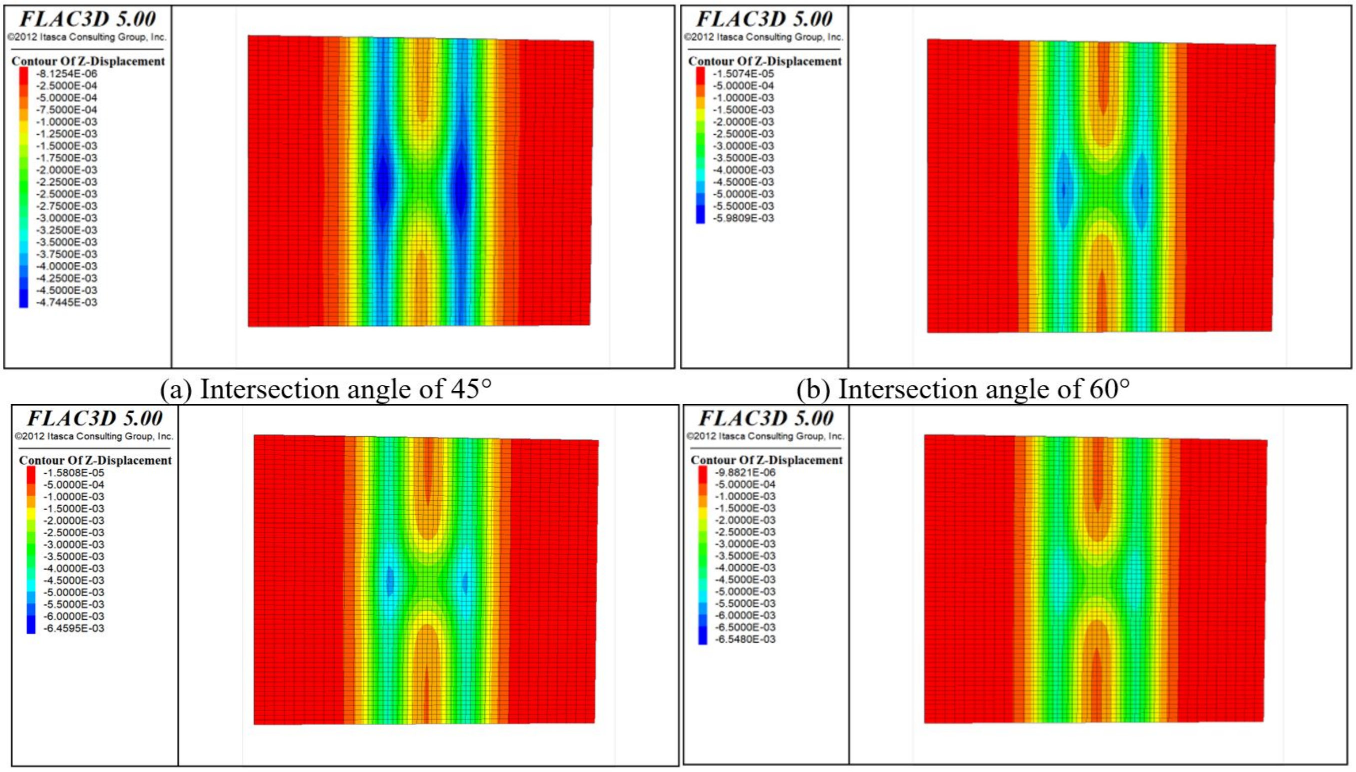


(a) Intersection angle of 45° (b) Intersection angle of 60°

(c) Intersection angle of 60° (d) Intersection angle of 90°

**Figure 12** Surface settlement under different intersection angles

Figure 13 shows the maximum settlement curves of the surface and cross passage at different intersection angles. Figure 14 shows the variation of the main tunnels at different intersection angles. As shown in Figure 13, the settlement of the cross passage vault decreases as the angle of the intersection increases. The linear correlation is significant. The maximum settlement of the surface increases first and then decreases with the increase of intersection angle, and the maximum value is obtained when the intersection angle is 75°. Similarly, the maximum settlement and convergence values of the main tunnels first increase and then decreases. As shown in Figure 14(a), the settlement and convergence of the main tunnels have minimum values when the intersection angle is 45°, and the maximum value is obtained when the intersection angle is 75°. The change rate of settlement of the main tunnels is 9.6%. The change rate of convergence of the main tunnels is 16.3%, which shows that the intersection angle considerably influences the horizontal convergence of the main tunnels.

Figure 14(b) shows that the maximum and minimum principal tensile and compressive stresses of the main tunnels also decrease as the intersection angle increases. However, the principal stress does not change considerably when the intersection angles are 75° and 90° and then stabilizes. This result is mainly due to the increase of intersection angle. The area of the intersection-affected zone rapidly decreases. The disturbance to the existing main tunnels also decreases. However, when the crossing angle is larger than 75°, the area affected by the intersection of the cross passage and main tunnels stabilizes and does not change remarkably. Therefore, the main stress of the main tunnels caused by construction stabilizes.

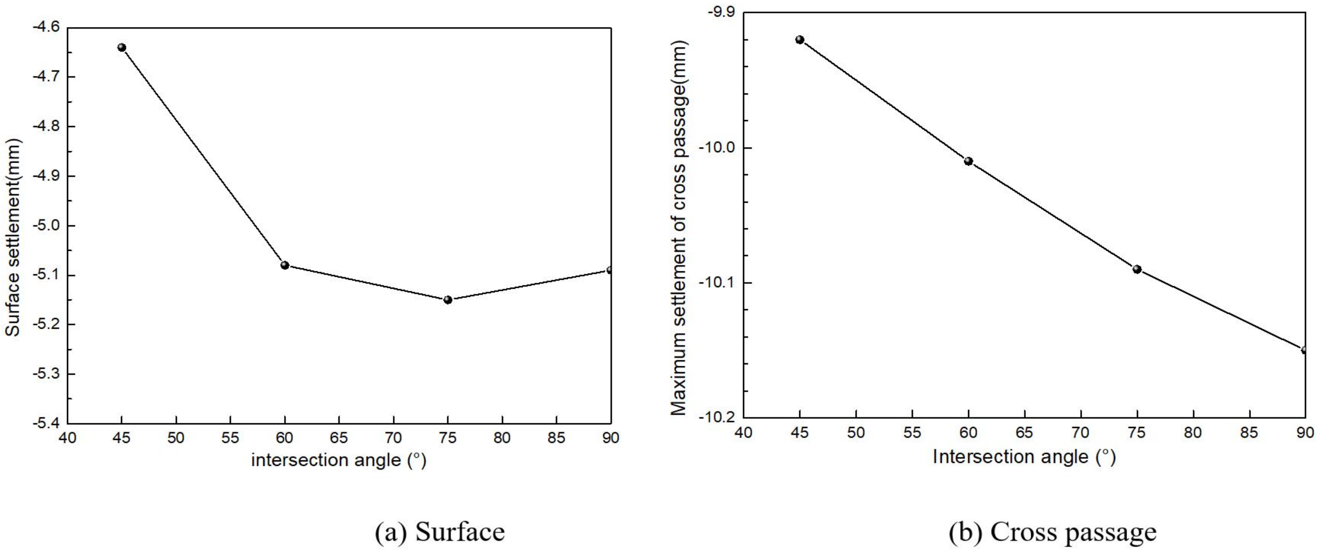


**Figure 13** Settlement of the surface and cross passage under different intersection angles

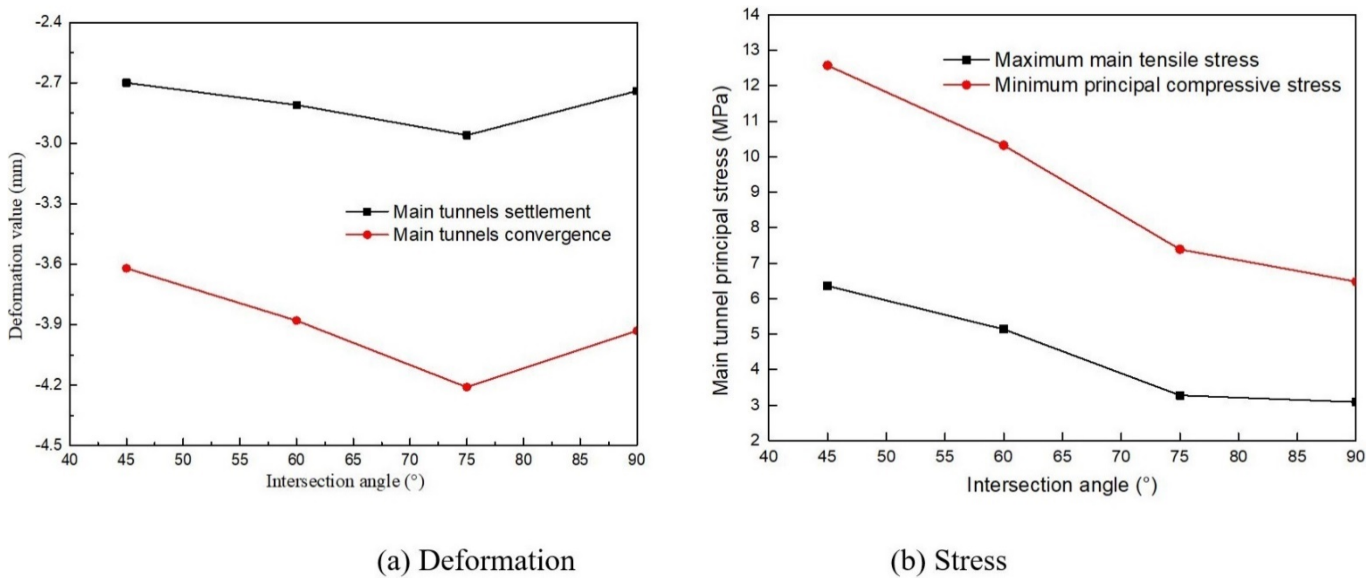


**Figure 14** Variation of the main tunnels under different intersection angles

### 4.3 Construction method

The influence of the construction of the cross passage on the settlement of the existing main tunnels is investigated by considering different construction methods. Working conditions under two different cross passage construction methods are calculated and analyzed. The specific operating condition parameters are shown in Table 10. For full-face excavation and benching tunneling construction method, the excavation is conducted from both sides with an excavation footage of 2 m.

**Table 10** Different excavation methods

| Working condition | Buried depth(m) | Intersection angle | Main tunnels type | Excavation method |
|---|---|---|---|---|
| **1** | 9 | 90° | Shield tunnel | full-face excavation |
| **2** | 9 | 90° | Shield tunnel | benching tunneling construction |

Figures 15 and 16 show that, after the cross passage excavation is completed, full-face excavation and benching tunneling construction show a certain uneven settlement. Surface settlement is observed along the axis of the main tunnels. The maximum uneven settlement of full-face excavation is 2.85 mm, and that of benching tunneling construction is 2.43 mm. Overall, the maximum settlement values of full-face excavation and benching tunneling construction are

5.09 and 4.34 mm, respectively. The maximum settlement value of benching tunneling construction is decreased by 14.7% compared with that of the full-face excavation. Therefore, the former shows better resistance, anti-sinking, and overall stability than the latter.

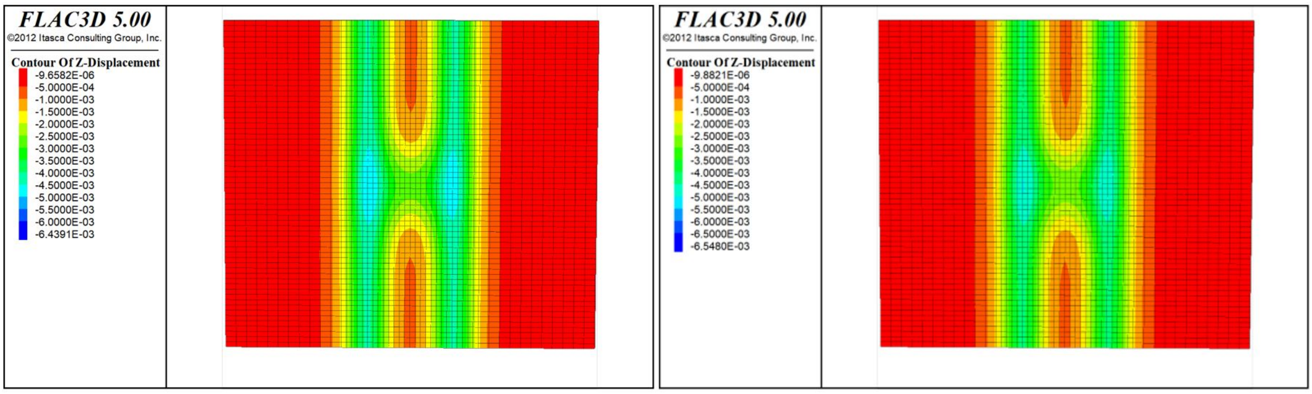


(a) Benching tunneling construction (b) Full-face excavation

**Figure 15** Surface settlement under different excavation methods

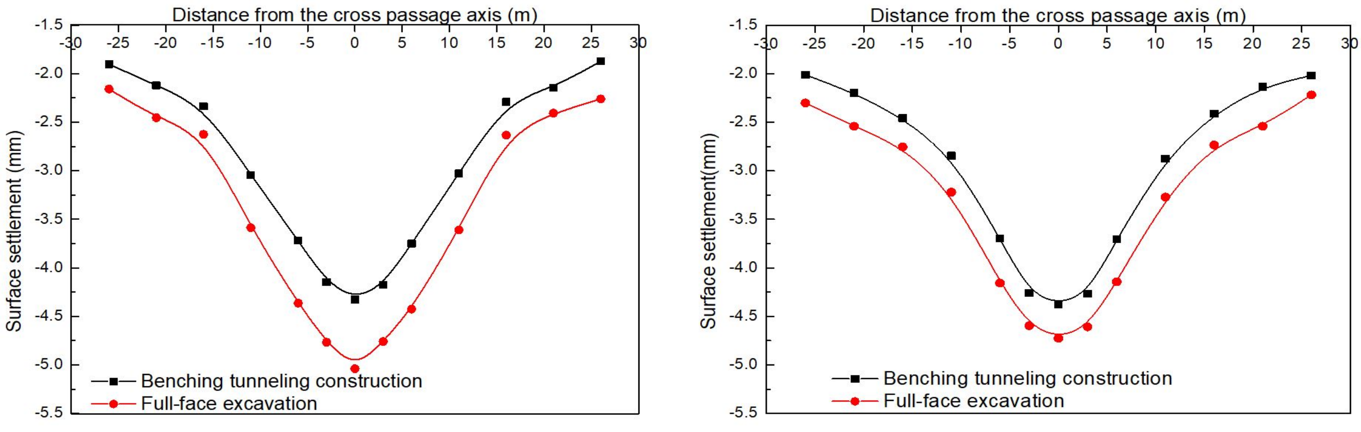


(a) Along the main tunnels axis (b) Along the centerline of the two main tunnels

**Figure 16** Surface settlement curve

The maximum and minimum principal stress distributions of the main tunnels are shown in Table 11. Overall, the stress distribution of the main tunnels under full-face excavation and benching tunneling construction has certain stress redistribution. However, the main stress value of the main tunnels under benching tunneling construction is less than that of the full-face excavation. The disturbance to the main tunnels by the former method is less than that by the latter method and thus shows better stability.

**Table 11** Principal stress of main tunnels (Mpa)

| Construction steps | Maximum tensile stress | Maximum principal compressive stress | Minimum principal compressive stress |
|---|---|---|---|
| **Initial stress** | 2.23 | 0.27 | 8.21 |
| **Step 1** | 2.33 / 2.46 | 0.29 / 0.32 | 8.21 / 8.22 |
| **Step 2** | 2.42 / 2.57 | 0.31 / 0.36 | 8.23 / 8.27 |
| **Step 3** | 2.49 / 2.63 | 0.33 / 0.40 | 8.31 / 8.37 |
| **Step 4** | 2.54 / 2.73 | 0.37 / 0.42 | 8.35 / 8.40 |

Note: The front and back "/" indicate the main stress values of benching tunneling construction and full-face excavation.

### 4.4 Grouting range

The grouting reinforcement of the following five working conditions is simulated by full-face excavation to compare and analyze the effect of grouting reinforcement. The cross passage is strengthened by advanced pre-grouting, as shown in Table 12.

**Table 12** Different grouting ranges

| Working condition | Buried depth | Intersection angle | Main tunnels type | Excavation method of cross passage | Grouting range (along the cross passage) |
|---|---|---|---|---|---|
| **1** | 9 m | 90° | Shield tunnel | full-face excavation | Not grouting |
| **2** | 9 m | 90° | Shield tunnel | full-face excavation | 2m on the left and right sides |
| **3** | 9 m | 90° | Shield tunnel | full-face excavation | 2m on the left and right sides and bottom |
| **4** | 9 m | 90° | Shield tunnel | full-face excavation | 2m on the left and right sides and the upper part |
| **5** | 9 m | 90° | Shield tunnel | full-face excavation | Reinforce 2m around |

The surface settlement and main tunnels variation curves along the main tunnels axis are shown in Figures 17 and 18, respectively. After the construction of the cross passage, the shape of the curve under each working condition is similar to "V" type, and the surface settlement reaches the maximum value directly above the axis of the cross passage. The surface settlement under working condition 1 is the largest, followed by working conditions 2, 3, 4, and 5. Notably, working condition 1 is much larger than other working conditions. The maximum surface settlement without grouting reinforcement (working condition 1) is 5.09 mm. As the reinforcement range increases, the surface settlement decreases. The maximum surface settlement under working condition 5 is only 3.17 mm, which is 37.7% lower than that without grouting reinforcement (working condition 1). This finding shows that reasonable grouting can effectively reduce surface settlement. The difference in surface settlement between working conditions 4 and 5 is small. Figure 18 shows that the grouting can considerably reduce the influence on the main tunnels. However, the deformation amount and main stress value under different grouting ranges are inconsiderably different. Therefore, the grouting plan should be reasonably selected depending on the actual situation during construction to avoid material waste and cost increase caused by excess grouting.

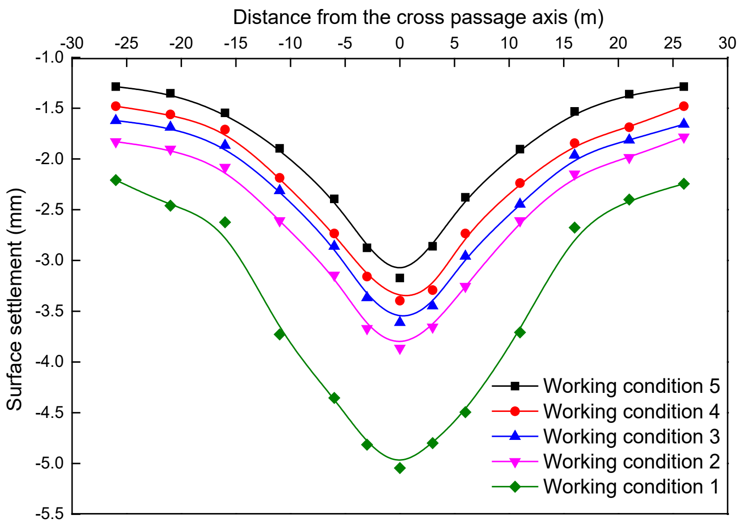


**Figure 17** Surface settlement curve along the main tunnels axis

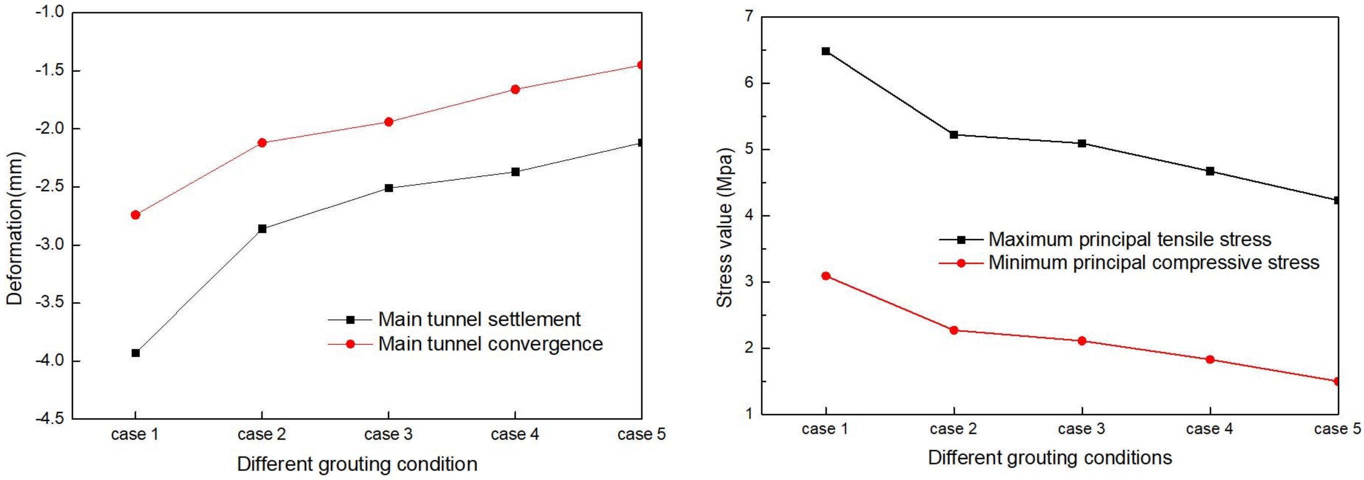

(a) Deformation (b) Stress

**Figure 18** Variation of the main tunnels under different grouting ranges

## 5 CONCLUSION

The mechanical characteristic analysis and influencing factors analysis of the cross passage construction are studied using FLAC3D. The main conclusions are summarized as follows.

(1) The construction of the cross passage largely disturbs the main tunnels. The settlement of the main tunnels is mainly concentrated from −7 to 7 m of the intersection of the main tunnels and cross passage. Therefore, these parts should be paid attention when conducting strengthening works.

(2) Stress concentration occurs in the intersecting segments. In particular, the open side panel has a disadvantageous form of pulling the entire upper and lower sections. Therefore, the segments near the cross passages should be strengthened effectively with sufficient support during construction.

(3) The construction of the cross passage causes a large tensile stress area in the structure. An unfavorable force form of intersection that is pulled up by the upper and lower sections is produced.

(4) The settlements of the surface and cross passage vault occur with the increase in buried depth. Similarly, the maximum and minimum principal stresses of the main tunnels also increase with the increase in the buried depth, and the linear correlation is significant.

(5) The maximum settlement of the surface increases first and then decreases with the increase in the intersection angle. The maximum and minimum principal tensile and compressive stresses of the main tunnels also decrease as the intersection angle increases. However, the principal stress at the intersection angles of 75° and 90° does not change considerably and stabilizes.

(6) The principal stress value of the main tunnels under benching tunneling construction is less than that of the full-face excavation. The former method shows better anti-sinking and overall stability than the latter.

(7) Reasonable grouting can effectively reduce surface settlement and disturbance to the main tunnels. The influence of different grouting reinforcement ranges is also small. Therefore, the grouting plan should be reasonably selected depending on the actual situation during construction to avoid material waste and cost increase caused by excess grouting.

**Author's Contributions:** Conceptualization, W Ke and C Shuaishuai; Methodology, W Ke; Investigation, W Ke, C Shuaishuai and Z Qianjin; Writing - original draft, C Shuaishuai, Z Qianjin and Z Zheng; Writing - review & editing, C Shuaishuai, Z Jiahui and Z Zheng; Funding acquisition, W Ke; Resources, W Ke, C Shuaishuai and Y Yalin; Supervision, W Ke.

**Editor:** Marcílio Alves

## References

[1].Wang T Z, Wang C M, Yao A J, et al. Vault Settlement Prediction for a Metro Cross Passage Based on Time Series [J]. Modern Tunnelling Technology, 2016, 53(3):74-81.

[2].Wang Z H, Li L Y, Wang G S, et al. Analysis of Mechanical Behaviors during Shield Launching Shaft Cross- Passage Construction in Soil/Rock Mixed Ground. [J]. Modern Tunnelling Technology, 2017, 54(3):82-89.

[3].Yan Q X, Chen C, Huang X, et al. Analysis on vibration response characteristics of cross structure between shield tunnels and cross passage induced by the train [J]. China Civil Engineering Journal, 2015(s1):228-235.

[4].Xia M Y, Li W, Feng X, et al. Grouting reinforcement and excavation stability on super-shallow buried and water-rich sand stratum subway cross passage [J]. Journal of Shandong University of Technology, 2017, 47(2):47-54.

[5].Murakami, H., Koizumi, A., 1980. On the behaviour of the transverse joints of a segment. In: The 35th Annual Conference of the JSCE, pp. 73–86. (in Japanese).

[6].E. Pimentel, S. Papakonstantinou, G. Anagnostou, Numerical interpretation of temperature distributions from three ground freezing applications in urban tunnelling, Tunn. Undergr. Space Technol. 28 (2011) 57–69.

[7].Han L, Guanlin Y E, Yuan-Hai L I, et al. In-situ monitoring of frost heave pressure during cross passage construction using ground freezing method[J]. Canadian Geotechnical Journal, 2016, 53(3).

[8].Yi K H, Tong S Y M. Cross passage mining in highly permeable and soft ground[J]. Japanese Geotechnical Society Special Publication, 2016, 2(75):2581-2584.

[9].Wang D, Gao Z, Lee J L, et al. Assessment and Optimization of Soil Mixing and Umbrella Vault Applied to a Cross-Passage Excavation in Soft Soils[J]. International Journal of Geomechanics, 2013, 14(6):04014027.

[10].Yi K H, Tong S Y M. Construction experiences from cross passage in very hard rock and blasting works near segmental lining[C]// World Tunnel Conference. 2015.

[11].Hu X D, Ji B Y. Optimization of Double-Ring-Pipe Freezing Scheme for Tunnel Cross-Passage Construction[J]. Advanced Materials Research, 2012, 446-449:2262-2266.

[12].Hu X D, Han Y G. Properties of Frozen Soils for Cross Passage Construction in Line 1 and 2 of Wuxi Metro[J]. Applied Mechanics & Materials, 2013, 353-356(353-356):1662-1665.

[13].Yan Q, Xu Y, Yang W, et al. Nonlinear transient analysis of temperature fields in an AGF project used for a cross-passage tunnel in the Suzhou Metro[J]. Ksce Journal of Civil Engineering, 2017, 22(3):1-11.

[14].Alhaddad M, Murro V D, Acikgoz S, et al. Photogrammetric and conventional deformation monitoring of an existing tunnel while a new cross-passage tunnel is excavated through its concrete lining for AWAKE project at CERN[C]// Chsm. 2016.

[15].Zeng H B, Wang Q S, Dong Z Q, et al. Study on Ground Settlement Law Caused by Excavation of π Type Double Cross passage[J]. Chinese Journal of Rock Mechanics and Engineering, 2018(s1).

[16].Liu J, He M D, Song H Y. Mechanical behaviors of shield tunnel segments due to construction of cross passages [C]// Chinese Journal of Geotechnical Engineering. 2013.

[17].Yang W. Risk Control Technology of Confined Water for Subway Passageway under River Bottom [J]. Building Construction, 2011, 33(7):616-617.

[18].Wang S M, He C, Gao Y L. Construction Mechanics Behavior of Interconnecting Aisle and Sump Pit of Shield Tunnel under High Hydraulic Pressure [J]. Journal of the China railway Society, 2012, 34(7):108-114.

[19].Li Z, Soga K, Wright P. Long-term performance of cast-iron tunnel cross passage in London clay[J]. Tunnelling & Underground Space Technology Incorporating Trenchless Technology Research, 2015, 50:152-170.